

# Ocular Safety of Intravitreal Propranolol and Its Efficacy in Attenuation of Choroidal Neovascularization

Ramin Nourinia,<sup>1</sup> Mozghan Rezaei Kanavi,<sup>1</sup> Amir Kaharkaboudi,<sup>1</sup> Seyed Iman Taghavi,<sup>2</sup> Seyed Javid Aldavood,<sup>2</sup> Soesiawati R. Darjatmoko,<sup>3</sup> Shoujian Wang,<sup>3</sup> Zafer Gurel,<sup>3</sup> Jeremy A. Lavine,<sup>3</sup> Sare Safi,<sup>1</sup> Hamid Ahmadih,<sup>4</sup> Narsis Daftarian,<sup>1</sup> and Nader Sheibani<sup>3,5</sup>

<sup>1</sup>Ocular Tissue Engineering Research Center, Shahid Beheshti University of Medical Sciences, Tehran, Iran

<sup>2</sup>Department of Clinical Sciences, Faculty of Veterinary Medicine, University of Tehran, Tehran, Iran

<sup>3</sup>Department of Ophthalmology and Visual Sciences, University of Wisconsin School of Medicine and Public Health, Madison, Wisconsin, United States

<sup>4</sup>Ophthalmic Research Center, Shahid Beheshti University of Medical Sciences, Tehran, Iran

<sup>5</sup>McPherson Eye Research Institute, University Wisconsin School of Medicine and Public Health, Madison, Wisconsin, United States

Correspondence: Nader Sheibani, Department of Ophthalmology and Visual Sciences, University of Wisconsin School of Medicine and Public Health, 1111 Highland Avenue, 9453 WIMR, Madison, WI 53705-2275, USA; nsheibanikar@wisc.edu.

Hamid Ahmadih, Ophthalmic Research Center, Shahid Beheshti University of Medical Sciences, No. 23, Paidarfard St. Boostan 9 St. Pasdaran Avenue, Tehran 16666, Iran; hahmadih@hotmail.com.

Submitted: April 24, 2015

Accepted: November 20, 2015

Citation: Nourinia R, Rezaei Kanavi M, Kaharkaboudi A, et al. Ocular safety of intravitreal propranolol and its efficacy in attenuation of choroidal neovascularization. *Invest Ophthalmol Vis Sci*. 2015;56:8228-8235. DOI:10.1167/iovs.15-17169

**PURPOSE.** Determine the safe dose of intravitreal propranolol (IVP), and evaluate its inhibitory effect on laser-induced choroidal neovascularization (CNV).

**METHODS.** To determine the IVP safe dose, 32 rabbits were divided into 4 groups. Three of these groups received IVP (15  $\mu$ L) corresponding to 15  $\mu$ g (group B), 30  $\mu$ g (group C), and 60  $\mu$ g (group D). The control group (A) received 15  $\mu$ L saline. Safety was assessed by ocular examination, electroretinography (ERG), routine histopathologic evaluation, immunohistochemistry for glial fibrillary acidic protein (GFAP), and real-time qPCR for GFAP, VEGF, thrombospondin 1 (TSP1), and pigment epithelium-derived factor (PEDF). A similar experiment was performed in 24 mice by using a 100-fold lower amount of propranolol (0.15, 0.3, and 0.6  $\mu$ g in 2  $\mu$ L) based on vitreous volume. For assessment of the angioinhibitory effects of IVP, CNV was induced in 42 mice via laser burns. Mice were divided into two groups: group 1 received the safe dose of IVP (0.3  $\mu$ g in 2  $\mu$ L) and group 2 received saline. Neovascularization area was quantified by intercellular adhesion molecule (ICAM)-2 immunostaining of choroidal-scleral flat mounts by using ImageJ software.

**RESULTS.** According to clinical, ERG, and histopathologic findings, 30  $\mu$ g IVP was chosen as the safe dose in rabbit eyes, comparable to 0.3  $\mu$ g IVP in mouse eyes. As compared to the control eyes, the development of CNV was attenuated (4.8-fold) in mice receiving 0.3  $\mu$ g IVP.

**CONCLUSIONS.** Intravitreal propranolol injection up to the final dose of 30  $\mu$ g in rabbits and 0.3  $\mu$ g in mice was safe, and was effective in attenuation of CNV in mice.

**Keywords:** choroidal neovascularization, intravitreal injections, propranolol, electroretinography, glial fibrillary acidic protein

Choroidal neovascularization (CNV) is a major cause of visual loss especially in the elderly. Recent studies<sup>1,2</sup> have established a key role for increased production of vascular endothelial growth factor (VEGF) in the development and progression of CNV. Vascular endothelial growth factor is secreted from the basal side of the retinal pigment epithelium (RPE) toward the choroid, and high levels of VEGF receptors, such as kinase insert domain receptor (KDR/VEGFR2) and fms-related tyrosine kinase-4 (FLT-4/VEGFR3), are found on the choriocapillaris endothelium facing the RPE layer.<sup>3,4</sup> Although overexpression of VEGF in RPE cells is sufficient to induce CNV in rats, the role of other regulatory factors in the pathogenesis of human CNV cannot be excluded.<sup>1,5-7</sup>

Propranolol is a nonselective  $\beta$ -adrenergic receptor ( $\beta$ -AR) blocking agent that specifically competes with  $\beta$ -AR agonists such as epinephrine and norepinephrine at the  $\beta$ 1- or  $\beta$ 2-AR sites.<sup>8</sup> An in vitro study<sup>9</sup> has shown that propranolol inhibits angiogenesis via attenuation of proliferation, migration, and differentiation of endothelial cells. Furthermore, this study reports that propranolol inhibits VEGF overexpression and

decreases induction of tyrosine phosphorylation of VEGFR-2; this inhibits activation of the extracellular signal-regulated kinase-1/2 and secretion of the extracellular matrix-degrading enzyme matrix metalloproteinase (MMP)-2. Other studies<sup>10,11</sup> have also demonstrated that propranolol and other  $\beta$  blockers dose-dependently reduce upregulated VEGF and decrease hypoxic levels of insulin growth factor-1 (IGF-1) mRNA and hypoxia-inducible factor-1 (HIF-1), which are necessary for new vessel formation.

Multiple case studies have reported that systemic propranolol could decrease the size of orbital hemangiomas.<sup>12,13</sup> In addition, a few studies<sup>11,14</sup> have demonstrated that systemic prescription of propranolol has antiangiogenic effects and could inhibit retinal and choroidal neovascularization in animal models. To increase ocular local delivery of propranolol and reduce its potential systemic toxicity, the present study was conducted to determine the safe dose of intravitreal propranolol (IVP) in rabbits and mice, and to assess its inhibitory effect in a mouse model of laser-induced CNV.

## METHODS

### Study Design

A two-phase study was designed to identify the maximum safe dose of IVP injection in rabbits and mice and to evaluate the possible inhibitory effect of IVP in a mouse laser-induced CNV model. All animal experiments were conducted in accordance with the Association for Research in Vision and Ophthalmology Statement for the Use of Animals in Ophthalmic and Vision Research and were approved by the Institutional Animal Care and Use Committee of the University of Wisconsin School of Medicine and Public Health and the Shahid Beheshti University of Medical Sciences. Animals were housed on a 12-hour light-dark cycle, with food and water provided ad libitum. Intramuscular injection of ketamine (80 mg/kg) and xylazine (10 mg/kg) was used for anesthesia. To induce pupillary dilation, 1% topical tropicamide was used.

### Phase I

Thirty-two female New Zealand white rabbits weighing approximately 1.5 kg were divided into four groups; each group included eight rabbits receiving intravitreal injections in their right eyes. The groups B, C, and D received a single IVP (15  $\mu$ L) injection corresponding to doses of 15, 30, and 60  $\mu$ g, respectively. The control group (group A) received 15  $\mu$ L normal saline. Injections were performed under sterile conditions with a surgical microscope by an expert ophthalmologist who was masked to the study. Ophthalmic examinations for intraocular inflammation, cataract formation, and retinal damage, and electroretinography (ERG) investigations were performed at baseline and on days 7 and 28 after injections. Finally, animals were euthanized and the enucleated eyes were processed for routine histopathologic evaluations and glial fibrillary acidic protein (GFAP) immunostaining. From clinical, ERG, and histopathologic data, the maximum safe dose of IVP was estimated for phase II of the study. To confirm that the selected doses are appropriate for preclinical evaluations in a mouse model of CNV, a similar experiment, excluding ERG analysis, was performed in 24 C57BL/6J mice. Mice were randomized into four groups, three of which (groups II–IV) received a single IVP injection (2  $\mu$ L) of 0.15, 0.3, and 0.6  $\mu$ g, respectively, corresponding to doses of 15, 30, and 60  $\mu$ g in rabbits, determined on the basis of approximate volume of vitreous in mice and rabbits. The control (group I) received 2  $\mu$ L saline. Mice received the same injections in both eyes; right eyes were used for histologic evaluations and left eyes were used for RNA isolation and qPCR analysis (see below).

**Electroretinography in Rabbits.** Animals were dark adapted for 12 hours, and all the following preparations were carried out under dim red illumination. Baseline ERGs were recorded just after injections. After intramuscular injection of ketamine and xylazine for anesthesia, pupil was dilated with 1% topical tropicamide. The body temperature of animals was kept constant during the ERG recording by placing the animals on a warmed platform (38°C). A ground electrode was fitted subcutaneously in the base of the tail and two reference electrodes were placed into the subcutaneous tissue behind the ears. A gold-wire electrode (Roland Consult, Brandenburg, Germany) internally covered with one drop of 2% methylcellulose gel (EyeGel; Eyeol, Dunstable, UK) was positioned to touch the central cornea. Again, rabbits were dark adapted for 10 minutes and scotopic recordings were made by using scotopic flash ERG at light intensities of 3 and 10 cd.s/m<sup>2</sup>. After 10 minutes of light adaptation, photopic cone responses were recorded by use of a photopic flash ERG at light intensity of 3 cd.s/m<sup>2</sup>. The analogue filters of the ERG device were set to the

frequency ranges of 0.5 to 200 Hz for both scotopic and photopic flash ERGs.

**Histopathology and Immunohistochemistry.** Animals were euthanized and the enucleated eyes were fixed in 10% formalin. Eyes were bisected axially and processed before embedding into paraffin blocks. Thin tissue sections at five different tissue planes (200  $\mu$ m apart) were prepared and stained with hematoxylin-eosin. Immunohistochemical staining for GFAP (Z 0334; Dako, Glostrup, Denmark) was also performed. The sections were examined under light microscopy (BX41; Olympus, Tokyo, Japan) by two masked ophthalmic pathologists for the presence of hemorrhage, inflammation, necrosis, and atrophy in the retina.

The results of GFAP immunoreactivity were scored by two ocular pathologists masked to the treated specimens on a scale from 0 to 5: 0, no staining; 1, staining limited to internal limiting membrane and nerve fiber layer; 2, focal staining of Müller cells involving partial length of the cells; 3, diffuse staining of Müller cells involving partial length of the cells; 4, focal staining of Müller cells involving full length of the cells; and 5, diffuse staining of Müller cells involving full length of the cells. Mean score > 2.5 in each study group was considered significant. Moreover, mean scores were compared between the groups.

**Preparation of RNA and qPCR Analysis.** The left eyes from mice receiving saline or different amounts of propranolol were enucleated and retinas were used for isolation of total RNA. Retinas (one pair) were homogenized in 1 mL Trizol (Life Technologies, Carlsbad, CA, USA). First, 0.2 mL chloroform was added to each sample, followed by vortexing for 20 seconds, and incubated at room temperature for 2 to 3 minutes. Samples were centrifuged at 16,000g for 20 minutes at 4°C and the aqueous phase (top) was transferred to a new tube. An equal volume of 100% RNase-free ethanol was added to each sample, and samples were loaded onto an RNeasy column (Qiagen, Valencia, CA, USA) and centrifuged for 30 seconds at 8000g. The flow-through was discarded and 700  $\mu$ L Buffer RW1 added to the column and centrifuged for 30 seconds at 8000g. Samples were washed twice with 500  $\mu$ L Buffer RPE. The columns were transferred to a new 1.5-mL collection tube and 40  $\mu$ L RNase-free water was added directly to the column membrane and incubated for 1 to 2 minutes at room temperature. RNA was eluted by centrifuging for 1 minute at 8000g. Complementary DNA (cDNA) synthesis was performed from 1  $\mu$ g total RNA by using Sprint RT Complete-Double PrePrimed Kit (Clontech, Mountain View, CA, USA) as recommended by the supplier. For qPCR, 1  $\mu$ L of each cDNA (1:10 dilution) was used as template in qPCR assays, performed in triplicate on Mastercycler Realplex (Eppendorf, Hauppauge, NY, USA) by using the SYBR qPCR Premix (Clontech) with specific primers: Gfap-F (AGGGACAACCTTGCACAGGA), Gfap-R (CAGCCTCAGGTT GGTTCAT), Pedf-F (GCCCAGAT GAAAGGGAAGATT), Pedf-R (TGAGGGCACTGGGCATTT), RpL13A-F (TCTCAAGGTTGTTCCGGCTGAA), RpL13A-R (GCCA GACGCC CCAGGTA), Tsp1-F (TGGCCAGCGTTGCCA), Tsp1-R (TCTGCAGCACCCCTGAA), Vegf-F (GGAGAGCAGAAGTCC CATGA), and Vegf-R (ACTCCAGGGCTTCATCGTTA). Amplification parameters were as follows: 95°C for 2 minutes, 40 cycles of amplification (95°C for 15 seconds, 60°C for 40 seconds), and dissociation curve step (95°C for 15 seconds, 60°C for 15 seconds, 95°C for 15 seconds). The linear regression line for nanogram of DNA was determined from relative fluorescent units at a threshold fluorescence value (Ct) to gene targets from retina extracts and normalized by the simultaneous amplification of *RpL13A* (a housekeeping gene) for all samples. Mean and standard deviation of all experiments performed were calculated after normalization to *RpL13A*.

## Phase II

**Laser-Induced CNV and Its Measurement.** Forty-two C57BL/6J mice were selected for the second phase of the study. Rupture of the Bruch's membrane was induced in the right eye of each mouse via laser. Briefly, after general anesthesia and pupillary dilation, three bursts of a 532-nm diode laser (spot size, 100  $\mu$ m; duration, 0.1 second; power, 100–300 mW) were delivered to each retina in the 9-, 12-, and 3-o'clock meridians. The procedure was performed with a slit lamp delivery laser system and a round glass cover slip as a contact lens to view the signs of Bruch's membrane rupture as a bubble formation. Cases with extensive hemorrhage were excluded. The mice were then divided into two groups: (1) the treatment group ( $n = 21$ ) that received a single intravitreal injection of the maximum safe dose of propranolol (2  $\mu$ L; 0.3  $\mu$ g) set for mice in the right eyes and (2) the control group ( $n = 21$ ) that received a single intravitreal injection of saline (2  $\mu$ L) in the right eyes. Intravitreal injections were performed at the time of laser application. Mice were euthanized on day 28,<sup>15</sup> eyes were enucleated, and fixed in 4% paraformaldehyde at 4°C for 2 hours. To obtain the posterior sclerochoroidal eyecup, eyes were transferred to phosphate-buffered saline (PBS) and sectioned at the equator by using a stereoscopic zoom dissecting microscope (LABOMED, Luxeo 4Z No. 444000; Nightingale Sales, Inc., Fort Myers, FL, USA). After 1 hour of incubation in blocking buffer (20% fetal calf serum, 20% normal goat serum, and 0.01% Triton X-100 in PBS) at room temperature, the posterior eyecups were incubated with anti-intercellular adhesion molecule (ICAM)-2 (1:500 in blocking buffer, catalog No. 553326; BD Biosciences, San Jose, CA, USA) overnight at 4°C. The samples were then washed three times with PBS and incubated with the Cy-3 anti-rat secondary antibody (1:500 in blocking buffer; catalog No. 712-165-153; Jackson ImmunoResearch, West Grove, PA, USA) for 2 hours. Finally, the posterior eyecups were flattened by 5 to 6 relaxing radial incisions and mounted on a glass slide with VectaMount AQ (Vector Laboratories, Malvern, PA, USA). The CNV images were captured with an inverted microscope (Olympus TH4-200; Olympus, Tokyo, Japan) fitted with appropriate excitation and emission filters (Olympus U-RSL-T) and equipped with a digital camera (Olympus U-TV0.63xc). ImageJ software (ImageJ 1.48, <http://imagej.nih.gov/ij/>; provided in the public domain by the National Institutes of Health, Bethesda, MD, USA) was used to quantify the total area of CNV associated with each laser burn.

**Statistical Analysis.** One-way analysis of variance was used to test the differences between ERG findings of treatment and control eyes. This test was also used to compare mean scores of GFAP immune reactivity between the study groups. The significance of differences between two time schedules for each group was tested by using paired *t*-test. Means and standard deviations of the CNV area in each group were calculated. Statistical difference between the treatment and control groups was determined by using the Mann-Whitney test. *P* value less than 0.05 was considered statistically significant.

## RESULTS

### Phase I

Systemic delivery of propranolol has shown efficacy in inhibition of neovascularization in various models including CNV.<sup>14</sup> Although systemic delivery of propranolol results in its delivery into the eye, a significantly higher concentration of propranolol may be needed to reach its therapeutic level in the eye.<sup>16</sup> The higher systemic doses of propranolol may have

adverse effects.<sup>17</sup> Therefore, we determined the impact of intravitreal delivery propranolol and its potential ocular toxicity in rabbits and mice. Animals received a single intravitreal dose of propranolol representing different amounts of propranolol. Animals were subjected to regular eye examination at 7 and 28 days post injection. Ocular inflammation, cataract formation, and retinal damage were not observed in clinical examinations of rabbit and mice eyes receiving different doses of propranolol.

**Rabbit ERG Analysis.** Rabbits receiving different doses of propranolol were subjected to ERG analysis both at baseline and then after 7 and 28 days post injection. The Table shows the mean amplitudes of a- and b-waves of all groups at baseline and on days 7 and 28 post injection. In group D (the highest dose), the photopic a- and b-wave amplitudes were significantly decreased on day 28 compared with the baseline ( $P = 0.009$  and  $P = 0.005$ , respectively). Thus, the lower doses of propranolol had no significant effect on retinal function.

**Light Microscopy.** For histologic evaluations, animals were sacrificed at desired times post treatment and eyes were prepared as detailed in Methods. Histopathologic examinations revealed no evidence of retinal hemorrhage, inflammation, necrosis, or atrophy in the rabbit groups (Figs. 1A1–D1). The GFAP immunoreactivity was notably increased in group D (mean [SE], 4.14 [0.48]) that had received 60  $\mu$ g IVP, as compared with groups A (mean [SE], 1.38 [0.55]) (Figs. 1A2–D2), B (mean [SE], 2.00 [1.50]), and C (mean [SE], 2.50 [1.10]), which was statistically significant ( $P < 0.0001$ ,  $P < 0.003$ , and  $P < 0.022$ , respectively). Light microscopic results, correlating with the ERG outcomes, demonstrated retinal toxicity attributable to IVP injection with a dose of 60  $\mu$ g, but not with the doses of 15 and 30  $\mu$ g. There was no evidence of retinal toxicity in the histologic sections of the fellow (noninjected) eyes.

In the mice, light microscopic examinations disclosed focal atrophic changes of retinal layers in four of six eyes (66.7%) in group IV that received IVP injection of 0.6  $\mu$ g. The atrophic changes were focally observed in photoreceptor outer segments, outer nuclear layer, inner nuclear layer, and ganglion cell layer. Such microscopic changes were not evident in any of the other groups (groups I–III) of the mice (Figs. 2A1–D1). Despite prominent histopathologic changes in group IV, mean score of GFAP immunoreactivity was not significantly different in any of the groups I to IV (I: mean [SE], 0.68 [0.52]; II: mean [SE], 0.67 [0.52]; III: mean [SE], 0.83 [0.41]; and IV: mean [SE], 1.00 [0.01]) (Figs. 2A2–D2). However, the dose of 0.6  $\mu$ g IVP was considered toxic for mice retinas with reference to the marked retinal changes in routine histopathology in group IV. Histologic assessment of noninjected eyes was unremarkable in all eyes.

The expression of GFAP (glial marker), TSP1 and PEDF (antiangiogenic factors), and VEGF (proangiogenic factor) were also determined by qPCR analysis. Figure 3A shows a modest increase in GFAP levels in the retinas from mice receiving 0.3 and 0.6  $\mu$ g propranolol, with the highest expression observed in the 0.6- $\mu$ g dose. These results are consistent with immunohistochemically detected GFAP in histologic sections from rabbit and mice eyes (Figs. 1, 2). We observed no dramatic change in VEGF expression in retinas from mice receiving 0.3 or 0.6  $\mu$ g propranolol. However, a modest increase was observed at 0.15  $\mu$ g propranolol (Fig. 3B). The TSP1 level was increased in retinas with 0.3  $\mu$ g propranolol, and no additional increase was noted with 0.6  $\mu$ g propranolol (Fig. 3C). The expression of PEDF did not change with various amounts of propranolol (Fig. 3D).

### Phase II

Considering the results of phase I study, the dose of 0.3  $\mu$ g IVP in mice eyes, corresponding to the dose of 30  $\mu$ g in rabbit eyes,

Investigative Ophthalmology & Visual Science

TABLE. Comparison of ERG Results Between the Groups in Phase I

	Groups												P Value
	Normal Saline (A)			15 µg/µL (B)			30 µg/µL (C)			60 µg/µL (D)			
	Mean ± SD	Med (Min, Max)		Mean ± SD	Med (Min, Max)		Mean ± SD	Med (Min, Max)		Mean ± SD	Med (Min, Max)		
<b>a-Wave</b>													
Scotopic, 3 cd.s/m <sup>2</sup>													
Pre injection	82.89 ± 21.92	85 (38.9, 119)		77.33 ± 32.64	84.1 (11.4, 118)		70.14 ± 15.64	71.35 (38.9, 95.3)		60.06 ± 15.81	60.85 (37.9, 89.3)		0.06
Week 1	96.38 ± 17.5	101.5 (50.8, 124)		89.54 ± 8.51	92.1 (74.2, 100)		82.08 ± 35.31	90.15 (3.92, 121)		72.57 ± 22.66	74.4 (27.6, 112)		0.058
Week 4	73.62 ± 19.36	69.05 (51, 112)		81.07 ± 16.33	83.35 (51.1, 106)		87.83 ± 28.65	100.35 (27.7, 112)		67.13 ± 19.63	61.75 (38.4, 101)		0.062
P within	0.09			0.197			0.254			0.233			
Scotopic, 10 cd.s/m <sup>2</sup>													
Pre injection	84.59 ± 38.05	91.35 (10.5, 133)		93.44 ± 22.16	93.4 (52.1, 126)		88.29 ± 15.33	87.6 (61.3, 111)		75.02 ± 15.25	76.45 (54.4, 109)		0.056
Week 1	113.7 ± 15.3	119 (72.4, 130)		107.11 ± 12.49	111 (75.5, 120)		93.33 ± 40.9	103.5 (2.72, 140)		87.28 ± 22.78	95.2 (30.8, 113)		0.018
Week 4	91.71 ± 18.42	86.75 (62.2, 125)		95.48 ± 15.7	94.9 (73.4, 131)		99.23 ± 29.22	104.5 (48.7, 142)		77.87 ± 22.43	75.5 (37.1, 113)		0.196
P within	<0.001			0.066			0.618			0.083			
<b>Photopic, 3 cd.s/m<sup>2</sup></b>													
Pre injection	13.84 ± 7.64	14.25 (2.31, 24.3)		13.98 ± 6.6	12.3 (2.91, 26.9)		9.89 ± 4.82	10.4 (2.48, 18.1)		15.41 ± 5.71	13.45 (8.18, 26.5)		0.002
Week 1	23.63 ± 35.5	10.01 (1, 119)		16.57 ± 5.86	16.6 (7.78, 26.6)		12.39 ± 6.83	11.4 (2.07, 23.7)		13.15 ± 6.68	13.1 (1.59, 21.8)		0.2
Week 4	14.1 ± 6.75	12.2 (6.91, 27.3)		14.08 ± 6.88	13.25 (4.43, 29.7)		12.83 ± 6.56	14.5 (3.4, 22.3)		9.02 ± 3.52	8.98 (1.43, 13.8)		0.963
P within	0.649			0.124			0.371			0.009			
<b>b-Wave</b>													
Scotopic, 3 cd.s/m <sup>2</sup>													
Pre injection	155.17 ± 39.95	153 (106, 211)		166 ± 48.6	169.5 (18, 249)		156.21 ± 33.72	165.5 (88.9, 196)		130.01 ± 27.98	125 (87.9, 184)		0.044
Week 1	160.56 ± 37.36	172 (80.7, 209)		194 ± 49.04	199.5 (122, 276)		167.84 ± 71.24	183.5 (8.88, 241)		136.68 ± 40.11	136.5 (58.5, 204)		0.013
Week 4	160.43 ± 39.51	165.5 (98.3, 229)		178.44 ± 46.21	174.5 (116, 274)		171.44 ± 61.63	182 (75.5, 254)		127.23 ± 34.3	135.5 (61.3, 185)		0.005
P within	0.836			0.156			0.716			0.818			
Scotopic, 10 cd.s/m <sup>2</sup>													
Pre injection	163.58 ± 41.64	169 (102, 223)		221.88 ± 85.1	196 (145, 516)		177.08 ± 40.45	176.5 (95.2, 253)		146.81 ± 29.92	145 (100, 216)		0.005
Week 1	188.42 ± 37.2	200.5 (104, 242)		220.19 ± 51.5	218 (102, 305)		185.96 ± 78.2	202 (6.18, 275)		156.39 ± 47.06	158.5 (45.5, 225)		0.005
Week 4	180.4 ± 35.43	177 (130, 234)		193.19 ± 46.53	184 (137, 296)		171.48 ± 63.06	191.5 (77.8, 234)		143.15 ± 41.95	149 (70.5, 207)		0.048
P within	0.342			0.067			0.903			0.616			
<b>Photopic, 3 cd.s/m<sup>2</sup></b>													
Pre injection	115.1 ± 20.6	116 (90.6, 141)		133.75 ± 25.19	136.5 (83.2, 167)		108.14 ± 38.11	112.5 (26.5, 174)		105.41 ± 33.35	111.5 (44, 162)		<0.001
Week 1	117.21 ± 30.65	118.5 (56.9, 161)		148.44 ± 28.12	143 (108, 194)		106.7 ± 56.7	111 (1.5, 186)		99.01 ± 26.56	102 (64.7, 139)		0.004
Week 4	125.98 ± 25.85	127 (86.3, 161)		138.93 ± 42.23	138 (63.8, 203)		119.84 ± 36.73	120.5 (68.5, 178)		75.44 ± 25.66	80.45 (26.1, 129)		0.037
P within	0.409			0.208			0.582			0.005			

P values are by generalized estimating equations. Mean amplitudes of a- and b-waves of all groups at baseline and days 7 and 28 were determined as described in Methods. P values for comparison between the groups at each time point are also shown. Intravitreal injections of propranolol with doses of 15 µg (group A), 30 µg (group B), and 60 µg (group C) were performed. The control group (D) received 15 µL normal saline. Max, maximum; Med, median; Min, minimum.

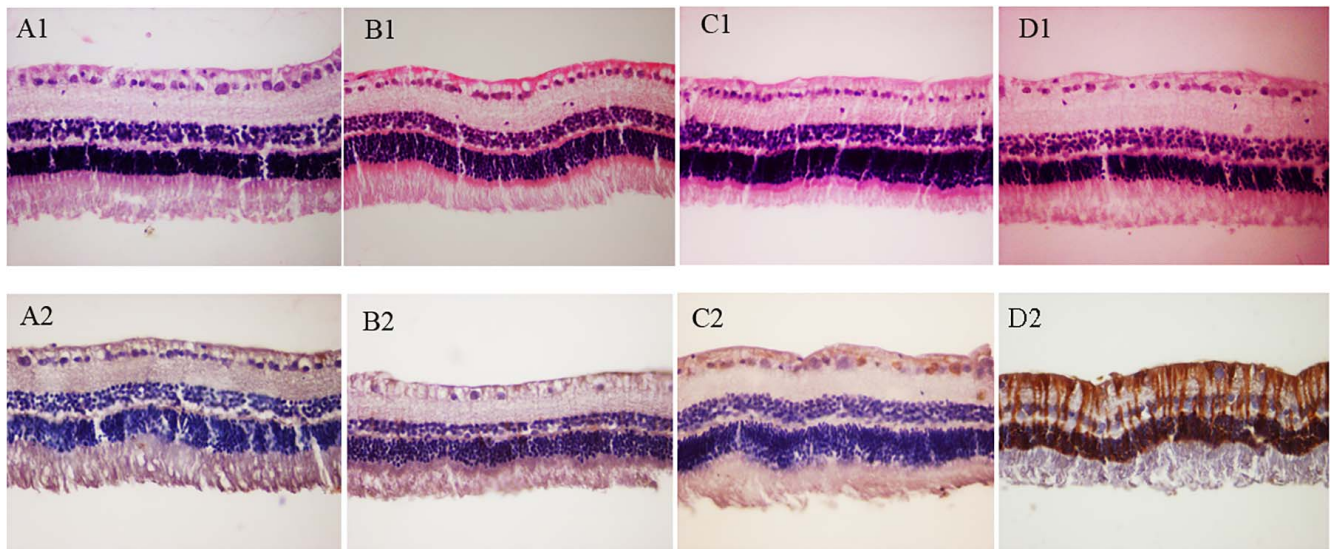


**FIGURE 1.** Representative unremarkable neurosensory retinas with 15  $\mu$ L intravitreal injection of 15  $\mu$ g (B1), 30  $\mu$ g (C1), and 60  $\mu$ g (D1) propranolol as compared to the normal saline-injected (A1) eyes (hematoxylin-eosin stain, magnification:  $\times 400$ ). Unremarkable immunoreactivity of the retina for GFAP in a representative eye injected with 15  $\mu$ g (B2) and 30  $\mu$ g (C2) propranolol. Please note remarkable retinal GFAP immunoreactivity in a representative eye injected with 60  $\mu$ g propranolol (D2) compared with that in a representative normal saline-injected (A2) eye (magnification:  $\times 400$ ). Please see the Results section for quantitative assessments of the data.

was selected for the phase II study evaluating the efficacy of intravitreal delivery of propranolol in a mouse model of laser-induced CNV. Four eyes from four mice in the CNV control group were phthisic at the time of enucleation and therefore were excluded. Mice eyes treated with 0.3  $\mu$ g IVP injection showed significantly smaller neovascular choroidal outgrowths (Figs. 4A, 4B) compared with the control. An approximately 4.8-fold decrease in the average CNV area was observed in the propranolol-treated group (mean [SE], 17,945 [25,971]  $\mu$ m<sup>2</sup>;  $n = 21$  eyes) compared with the control (mean [SE], 86821

[49,274]  $\mu$ m<sup>2</sup>;  $n = 17$  eyes), which was statistically significant ( $*P < 0.001$ ) (Fig. 4C).

## DISCUSSION

In this study IVP doses of 30 and 0.3  $\mu$ g were found to be safe when used in rabbit and mice eyes, respectively. This dose in the mouse eyes resulted in significant attenuation of neovascular outgrowth in the laser-induced CNV model. These results suggested that IVP, similar to its systemic administration,<sup>11,14</sup>

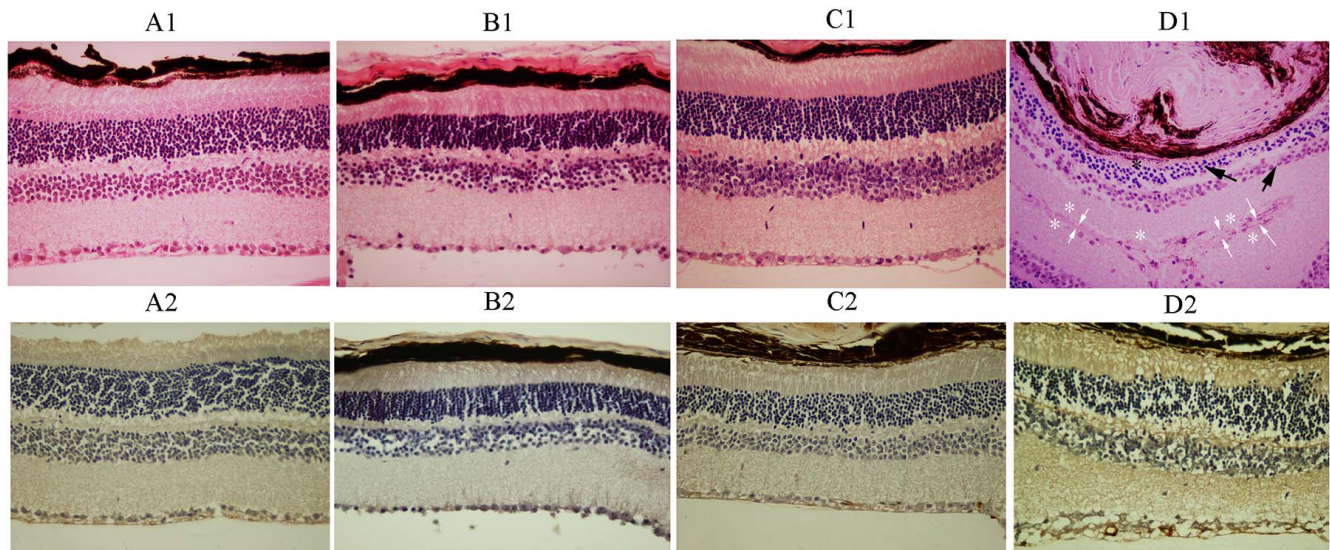


**FIGURE 2.** Representative histologic sections of neurosensory retinas in groups I to IV: (A1) group I, (B1) group II, (C1) group III, and (D1) group IV (hematoxylin-eosin stain, magnification:  $\times 400$ ). Please note unremarkable retinal layers in (A1), (B1), and (C1) in comparison to focal retinal atrophic changes in (D1). Please also note the presence of atrophic photoreceptor outer segments (*black asterisk*), atrophic changes in outer and inner nuclear layers (*black arrows*), and focal loss of ganglion cells (*white asterisks*) in a folded retina in (D1). *White arrows* demonstrate where the internal limiting membranes of the folded retina artifactually face each other. The GFAP immunoreactivity of the representative retinas in groups I to IV: (A2) group I, (B2) group II, (C2) group III, and (D2) group IV (magnification:  $\times 400$ ). No significant changes in GFAP immunoreactivity were detectable in the representative sections. Please see the Results section for quantitative assessments of the data.

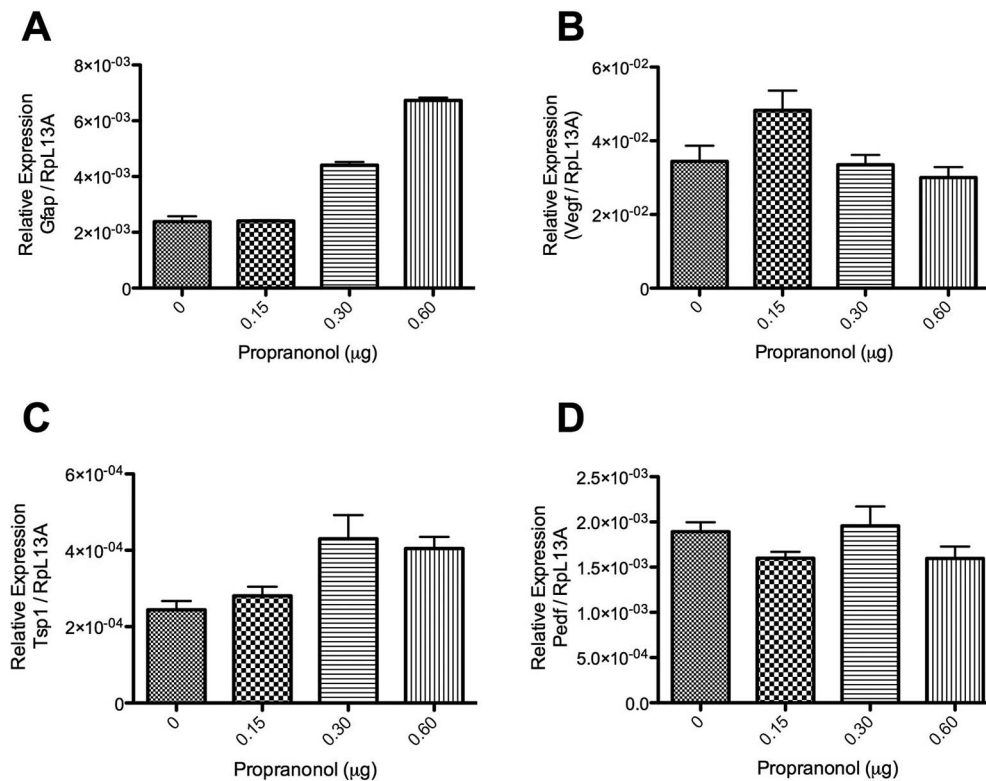


**FIGURE 3.** Quantitative assessment of GFAP (A), VEGF (B), TSP1 (C), and PEDF (D) expression in mouse eyes receiving different amounts of propranolol. The expression of desired genes was determined by qPCR and specific set of primers as detailed in the Methods. Please note a dramatic increase in the level of GFAP in retinas with 0.6 µg propranolol. The VEGF levels (all isoforms) were not affected at 0.3 µg propranolol, but a modest increase was detected in retinas with 0.15 µg propranolol. The level of TSP1 was increased at 0.3 µg propranolol but PEDF levels did not change.

had antiangiogenic properties and may be suitable as a new treatment modality for exudative age-related macular degeneration. Furthermore, with IVP injection the side effects of systemic route may be minimized as demonstrated with eye drop delivery of propranolol for treatment of retinal neovascularization.<sup>16,18</sup>

Intravitreal propranolol injection can provide a higher concentration of drug in the retina and choroid. In the study by Martini et al.,<sup>19</sup> after subcutaneous administration of 20 mg/kg propranolol three times daily, the concentration of propranolol in the retina was  $20.02 \pm 3.21$  µg/g. Whereas another study assessing the pharmacokinetics of propranolol in the isolated perfused ovine eye indicates that after 500 µg intravitreal injection of propranolol, the peak level of drug in the retina is 1240 ng/g only 3 hours after injection, and in the choroid a peak level of 4975 ng/g is obtained 7 hours after injection.<sup>20</sup> Thus, topical and intravitreal delivery of propranolol leads to significantly higher ocular levels, and its lower systemic levels may eliminate potential complications.<sup>16–18,21,22</sup>

Previous studies have demonstrated various results regarding the possible role of different β-ARs in retinal angiogenesis. In a study by Martini et al.,<sup>19</sup> β1 agonists do not affect angiogenic phenotype in human choroidal and retinal endothelial cells. Moreover, β1 blockade does not affect retinal levels of proangiogenic factors.<sup>19</sup> However, Dal Monte et al.<sup>23</sup> have shown that β1-AR may play a pivotal role in retinal angiogenesis.<sup>23</sup> Most studies<sup>11,19</sup> also indicate that β2-AR plays a key role in the angiogenic processes in CNV and oxygen-induced ischemic retinopathy (OIR). Steinle et al.<sup>24</sup> and Ristori et al.<sup>11</sup> have suggested that β3-ARs can also induce retinal endothelial cell proliferation and migration. Thus, additional studies using specific antagonists of β-AR and/or transgenic

mice lacking specific β-AR are needed to demonstrate the specific β-AR involved in these activities.

Propranolol as a nonselective β-blocker inhibits growth factor-induced endothelial cell proliferation, growth factor-induced migration, VEGF-induced MMP-2 secretion, and VEGF-induced tyrosine phosphorylation of VEGFR-2 in an in vitro study.<sup>9</sup> The authors<sup>9</sup> conclude that inhibitory effects of propranolol on angiogenesis affects not only β-AR signaling but also the inhibition of the VEGFR-2 pathway. Later studies<sup>11,19</sup> evaluating the inhibitory effects of systemic propranolol on neovascularization in mice models of OIR have indicated that the systemic administration of propranolol reduces retinal VEGF, IGF-1, retinal neovascularization, and vascular leakage.

We recently have demonstrated that intraperitoneal injection of propranolol ameliorates CNV size and decreases VEGF level via β2-AR blockade in various ocular cell types including RPE and choroidal endothelial cells.<sup>15</sup> Most interestingly, the basal level of VEGF is not affected by the β2-AR blockade, since basal VEGF expression and/or activity is essential for a number of systemic functions and neuronal integrity of the retina.<sup>14</sup> Thus, the use of β2-AR blockade may provide a specific mechanism to selectively reduce pathologic levels of VEGF without affecting the basal levels needed for normal tissue functions. Here we also observed an increase in the level of TSP1 in retinas with 0.3 µg propranolol, without a dramatic effect on the levels of VEGF. Thus, increased production of TSP1 by propranolol may also contribute to attenuation of CNV, as we have recently demonstrated with a TSP1 mimetic peptide.<sup>25</sup> The higher levels of VEGF at 0.15 µg propranolol, without a change in TSP1 level, suggest this dose of propranolol may not be as effective in blocking CNV and awaits further confirmation.

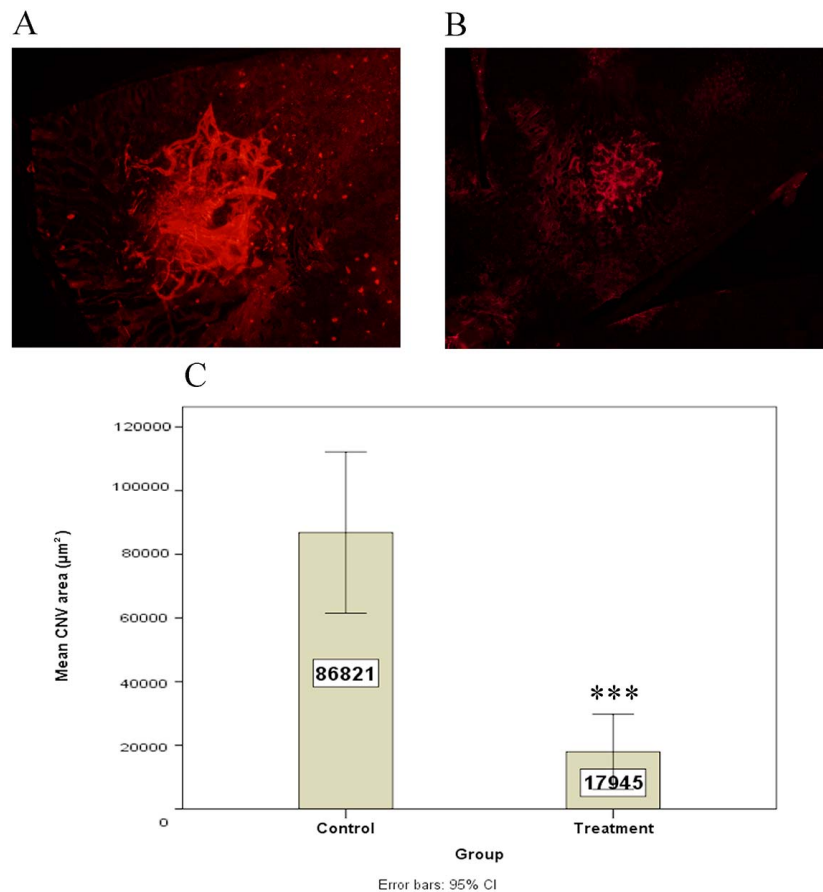


**FIGURE 4.** Attenuation of CNV following intravitreal administration of propranolol in the mouse laser-induced CNV model. Representative choroidal flat mounts after staining with ICAM-2, 4 weeks after laser photocoagulation, are shown. (A) Choroidal neovascularization in mice that received a single intravitreal injection of saline. (B) Choroidal neovascularization in mice that received a single intravitreal injection of propranolol. The quantification of the data is shown in (C). An approximately 5-fold decrease in the area of CNV was observed in mice that received IVP compared with controls ( $*P < 0.001$ ).

Multiple factors may be responsible for VEGF expression in CNV. Hypoxia seems to be the main factor for VEGF expression in retinal neovascularization, but it may not play a specific role in a vascular-rich background of the choroid and therefore in CNV. However, an important role for expression of HIF-1 in RPE cells and CNV has been demonstrated.<sup>26</sup> It is also possible that other factors such as age, insulin-like growth factor 1, inflammatory cytokines, transforming growth factor  $\beta$ ,<sup>1,5-7</sup> and adrenergic signaling contribute to VEGF expression in CNV. The results of our study with adrenergic blockade suggest adrenergic signaling is one of the specific contributors to alterations in the ocular angiogenic balance and CNV. However, the detailed mechanisms and the target cells involved remain the subject of future investigation.

One of the limitations of this study was the short follow-up time and knowledge of propranolol half-life during the phase I study. However, the results of ERG analysis demonstrated that a single injection of 60  $\mu\text{g}$  propranolol in rabbit eyes induced significant reduction of photopic a- and b-waves. This finding may indicate that IVP toxicity first affects cone photoreceptors, and longer follow-up is needed to assess the toxic effects of IVP on rod photoreceptors. Consistent with ERG results, the histologic evaluations showed early toxic effects without significant photoreceptor loss in 60- $\mu\text{g}$  and 0.6- $\mu\text{g}$  groups in the rabbits and mice, respectively. However, a longer follow-up may demonstrate more toxic effects. Therefore, future studies with longer follow-up times and multiple intravitreal propranolol

injections are needed to assess the long-term toxicity of this treatment.

In summary, the present study showed the safety of a single IVP injection of 30  $\mu\text{g}$  in rabbits and 0.3  $\mu\text{g}$  in mice. In addition, a single intravitreal delivery of 0.3  $\mu\text{g}$  propranolol in mice had a significant inhibitory effect on CNV. Further studies are required to confirm the efficacy of IVP, alone or as adjuvant to existing modalities, as an appropriate treatment for translation to human ocular neovascular disorders.

#### Acknowledgments

Supported by R24 EY022883 and P30 EY016665 from the National Institutes of Health, and an unrestricted departmental award from Research to Prevent Blindness (to NS). NS is a recipient of Alice R. McPherson-Retina Research Foundation Chair.

Disclosure: **R. Nourinia**, None; **M. Rezaei Kanavi**, None; **A. Kaharkaboudi**, None; **S.I. Taghavi**, None; **S.J. Aldavood**, None; **S.R. Darjatmoko**, None; **S. Wang**, None; **Z. Gurel**, None; **J.A. Lavine**, None; **S. Safi**, None; **H. Ahmadi**, None; **N. Daftarian**, None; **N. Sheibani**, None

#### References

- Spilbury K, Garrett KL, Shen WY, Constable IJ, Rakoczy PE. Overexpression of vascular endothelial growth factor (VEGF) in the retinal pigment epithelium leads to the development of choroidal neovascularization. *Am J Pathol.* 2000;157:135-144.

2. Ishibashi T, Hata Y, Yoshikawa H, Nakagawa K, Sueishi K, Inomata H. Expression of vascular endothelial growth factor in experimental choroidal neovascularization. *Graefes Arch Clin Exp Ophthalmol*. 1997;235:159-167.
3. Wada T, McKee MD, Steitz S, Giachelli CM. Calcification of vascular smooth muscle cell cultures: inhibition by osteopontin. *Circ Res*. 1999;84:166-178.
4. Blaauwgeers HG, Holtkamp GM, Rutten H, et al. Polarized vascular endothelial growth factor secretion by human retinal pigment epithelium and localization of vascular endothelial growth factor receptors on the inner choriocapillaris: evidence for a trophic paracrine relation. *Am J Pathol*. 1999;155:421-428.
5. Pepper MS, Ferrara N, Orci L, Montesano R. Potent synergism between vascular endothelial growth factor and basic fibroblast growth factor in the induction of angiogenesis in vitro. *Biochem Biophys Res Commun*. 1992;189:824-831.
6. Goto F, Goto K, Weindel K, Folkman J. Synergistic effects of vascular endothelial growth factor and basic fibroblast growth factor on the proliferation and cord formation of bovine capillary endothelial cells within collagen gels. *Lab Invest*. 1993;69:508-517.
7. Amin R, Puklin JE, Frank RN. Growth factor localization in choroidal neovascular membranes of age-related macular degeneration. *Invest Ophthalmol Vis Sci*. 1994;35:3178-3188.
8. Mak IT, Weglicki WB. Potent antioxidant properties of 4-hydroxyl-propranolol. *J Pharmacol Exp Ther*. 2004;308:85-90.
9. Lamy S, Lachambre MP, Lord-Dufour S, Beliveau R. Propranolol suppresses angiogenesis in vitro: inhibition of proliferation, migration, and differentiation of endothelial cells. *Vascul Pharmacol*. 2010;53:200-208.
10. Shyu KG, Liou JY, Wang BW, Fang WJ, Chang H. Carvedilol prevents cardiac hypertrophy and overexpression of hypoxia-inducible factor-1alpha and vascular endothelial growth factor in pressure-overloaded rat heart. *J Biomed Sci*. 2005;12:409-420.
11. Ristori C, Filippi L, Dal Monte M, et al. Role of the adrenergic system in a mouse model of oxygen-induced retinopathy: antiangiogenic effects of beta-adrenoreceptor blockade. *Invest Ophthalmol Vis Sci*. 2011;52:155-170.
12. Leaute-Labreze C, Dumas de la Roque E, Hubiche T, Boralevi F, Thambo JB, Taieb A. Propranolol for severe hemangiomas of infancy. *N Engl J Med*. 2008;358:2649-2651.
13. Taban M, Goldberg RA. Propranolol for orbital hemangioma. *Ophthalmology*. 2010;117:195-195.e194.
14. Lavine JA, Sang Y, Wang S, Ip MS, Sheibani N. Attenuation of choroidal neovascularization by beta2-adrenoreceptor antagonism. *JAMA Ophthalmol*. 2013;131:376-382.
15. Husain D, Meyer RD, Mehta M, et al. Role of c-Cbl-dependent regulation of phospholipase Cgamma1 activation in experimental choroidal neovascularization. *Invest Ophthalmol Vis Sci*. 2010;51:6803-6809.
16. Hao J, Yang MB, Liu H, Li SK. Distribution of propranolol in periocular tissues: a comparison of topical and systemic administration. *J Ocul Pharmacol Ther*. 2011;27:453-459.
17. Filippi L, Cavallaro G, Bagnoli P, et al. Oral propranolol for retinopathy of prematurity: risks, safety concerns, and perspectives. *J Pediatr*. 2013;163:1570-1577.e1576.
18. Dal Monte M, Casini G, la Marca G, Isacchi B, Filippi L, Bagnoli P. Eye drop propranolol administration promotes the recovery of oxygen-induced retinopathy in mice. *Exp Eye Res*. 2013;111:27-35.
19. Martini D, Monte MD, Ristori C, et al. Antiangiogenic effects of beta2-adrenergic receptor blockade in a mouse model of oxygen-induced retinopathy. *J Neurochem*. 2011;119:1317-1329.
20. Mains J, Tan LE, Wilson C, Urquhart A. A pharmacokinetic study of a combination of beta adrenoreceptor antagonists - in the isolated perfused ovine eye. *Eur J Pharm Biopharm*. 2012;80:393-401.
21. Liu H, Yang MB, Li SK, Hao J. Effects of dosing protocol on distribution of propranolol in periocular tissues after topical ocular instillation. *Curr Eye Res*. 2014;40:1-8.
22. Starkey E, Shahidullah H. Propranolol for infantile haemangiomas: a review. *Arch Dis Child*. 2011;96:890-893.
23. Dal Monte M, Cammalleri M, Mattei E, Filippi L, Bagnoli P. Protective effects of beta1/2 adrenergic receptor deletion in a model of oxygen-induced retinopathy. *Invest Ophthalmol Vis Sci*. 2014;56:59-73.
24. Steinle JJ, Booz GW, Meininger CJ, Day JN, Granger HJ. Beta 3-adrenergic receptors regulate retinal endothelial cell migration and proliferation. *J Biol Chem*. 2003;278:20681-20686.
25. Wang S, Sorenson CM, Sheibani N. Lack of thrombospondin 1 and exacerbation of choroidal neovascularization. *Arch Ophthalmol*. 2012;130:615-620.
26. Lin M, Hu Y, Chen Y, et al. Impacts of hypoxia-inducible factor-1 knockout in the retinal pigment epithelium on choroidal neovascularization. *Invest Ophthalmol Vis Sci*. 2012;53:6197-6206.